



First decay-time-dependent analysis of $B^0 \rightarrow K_s^0 \pi^0$ at Belle II

F. Abudinén, I. Adachi, R. Adak, K. Adamczyk, L. Aggarwal, P. Ahlburg, H. Ahmed, J. K. Ahn, H. Aihara, N. Akopov, A. Aloisio, F. Ameli, L. Andricsek, N. Anh Ky, D. M. Asner, H. Atmacan, V. Aulchenko, T. Aushev, V. Aushev, T. Aziz, V. Babu, S. Bacher, H. Bae, S. Baehr, S. Bahinipati, A. M. Bakich, P. Bambade, Sw. Banerjee, S. Bansal, M. Barrett, G. Batignani, J. Baudot, M. Bauer, A. Baur, A. Beaubien, A. Beaulieu, J. Becker, P. K. Behera, J. V. Bennett, E. Bernieri, F. U. Bernlochner, M. Bertemes, E. Bertholet, M. Bessner, S. Bettarini, V. Bhardwaj, B. Bhuyan, F. Bianchi, T. Bilka, S. Bilokin, D. Biswas, A. Bobrov, D. Bodrov, A. Bolz, A. Bondar, G. Bonvicini, A. Bozek, M. Bračko, P. Branchini, N. Braun, R. A. Briere, T. E. Browder, D. N. Brown, A. Budano, L. Burmistrov, S. Bussino, M. Campajola, L. Cao, G. Casarosa, C. Cecchi, D. Červenkov, M.-C. Chang, P. Chang, R. Cheaib, P. Cheema, V. Chekelian, C. Chen, Y. Q. Chen, Y.-T. Chen, B. G. Cheon, K. Chilikin, K. Chirapatpimol, H.-E. Cho, K. Cho, S.-J. Cho, S.-K. Choi, S. Choudhury, D. Cinabro, L. Corona, L. M. Cremaldi, S. Cunliffe, T. Czank, S. Das, N. Dash, F. Dattola, E. De La Cruz-Burelo, G. de Marino, G. De Nardo, M. De Nuccio, G. De Pietro, R. de Sangro, B. Deschamps, M. Destefanis, S. Dey, A. De Yta-Hernandez, R. Dhamija, A. Di Canto, F. Di Capua, S. Di Carlo, J. Dingfelder, Z. Doležal, I. Domínguez Jiménez, T. V. Dong, M. Dorigo, K. Dort, D. Dossett, S. Dreyer, S. Dubey, S. Duell, G. Dujany, P. Ecker, S. Eidelman, M. Eliachevitch, D. Epifanov, P. Feichtinger, T. Ferber, D. Ferlewicz, T. Fillinger, C. Finck, G. Finocchiaro, P. Fischer, K. Flood, A. Fodor, F. Forti, A. Frey, M. Friedl, B. G. Fulsom, M. Gabriel, A. Gabrielli, N. Gabyshev, E. Ganiev, M. Garcia-Hernandez, R. Garg, A. Garmash, V. Gaur, A. Gaz, U. Gebauer, A. Gellrich, J. Gemmler, T. Geßler, D. Getzkow, G. Giakoustidis, R. Giordano, A. Giri, A. Glazov, B. Gobbo, R. Godang, P. Goldenzweig, B. Golob, P. Gomis, G. Gong, P. Grace, W. Gradl, E. Graziani, D. Greenwald, T. Gu, Y. Guan, K. Gudkova, J. Guilleams, C. Hadjivasiliou, S. Halder, K. Hara, T. Hara, O. Hartbrich, K. Hayasaka, H. Hayashii, S. Hazra, C. Hearty, M. T. Hedges, I. Heredia de la Cruz, M. Hernández Villanueva, A. Hershenhorn, T. Higuchi, E. C. Hill, H. Hirata, M. Hoek, M. Hohmann, S. Hollitt, T. Hotta, C.-L. Hsu, Y. Hu, K. Huang, T. Humair, T. Iijima, K. Inami, G. Inguglia, N. Ipsita, J. Irakkathil Jabbar, A. Ishikawa, S. Ito, R. Itoh, M. Iwasaki, Y. Iwasaki, S. Iwata, P. Jackson, W. W. Jacobs, I. Jaegle, D. E. Jaffe, E.-J. Jang, M. Jeandron, H. B. Jeon, Q. P. Ji, S. Jia, Y. Jin, C. Joo, K. K. Joo, H. Junkerkalefeld, I. Kadenko, J. Kahn, H. Kakuno, M. Kaleta, A. B. Kaliyar, J. Kandra, K. H. Kang, P. Kapusta, R. Karl, G. Karyan, Y. Kato, H. Kawai, T. Kawasaki, C. Ketter, H. Kichimi, C. Kiesling, B. H. Kim, C.-H. Kim, D. Y. Kim, H. J. Kim, K.-H. Kim, K. Kim, S.-H. Kim, Y.-K. Kim, Y. Kim, T. D. Kimmel, H. Kindo, K. Kinoshita, C. Kleinwort, B. Knysh, P. Kodyš, T. Koga, S. Kohani, I. Komarov, T. Konno, A. Korobov, S. Korpar, N. Kovalchuk, E. Kovalenko, R. Kowalewski, T. M. G. Kraetzschmar, F. Krinner,

P. Križan, R. Kroeger, J. F. Krohn, P. Krokovny, H. Krüger, W. Kuehn, T. Kuhr,
 J. Kumar, M. Kumar, R. Kumar, K. Kumara, T. Kumita, T. Kunigo, M. Künzel,
 S. Kurz, A. Kuzmin, P. Kvasnička, Y.-J. Kwon, S. Lacaprara, Y.-T. Lai, C. La Licata,
 K. Lalwani, T. Lam, L. Lanceri, J. S. Lange, M. Laurenza, K. Lautenbach, P. J. Laycock,
 R. Leboucher, F. R. Le Diberder, I.-S. Lee, S. C. Lee, P. Leitl, D. Levit, P. M. Lewis,
 C. Li, L. K. Li, S. X. Li, Y. B. Li, J. Libby, K. Lieret, J. Lin, Z. Liptak, Q. Y. Liu,
 Z. A. Liu, D. Liventsev, S. Longo, A. Loos, A. Lozar, P. Lu, T. Lueck, F. Luetticke,
 T. Luo, C. Lyu, C. MacQueen, M. Maggiora, R. Maiti, S. Maity, R. Manfredi, E. Manoni,
 S. Marcello, C. Marinas, L. Martel, A. Martini, L. Massaccesi, M. Masuda, T. Matsuda,
 K. Matsuoka, D. Matvienko, J. A. McKenna, J. McNeil, F. Meggendorfer, F. Meier,
 M. Merola, F. Metzner, M. Milesi, C. Miller, K. Miyabayashi, H. Miyake, H. Miyata,
 R. Mizuk, K. Azmi, G. B. Mohanty, N. Molina-Gonzalez, S. Moneta, H. Moon, T. Moon,
 J. A. Mora Grimaldo, T. Morii, H.-G. Moser, M. Mrvar, F. J. Müller, Th. Muller,
 G. Muroyama, C. Murphy, R. Mussa, I. Nakamura, K. R. Nakamura, E. Nakano,
 M. Nakao, H. Nakayama, H. Nakazawa, M. Naruki, Z. Natkaniec, A. Natochii, L. Nayak,
 M. Nayak, G. Nazaryan, D. Neverov, C. Niebuhr, M. Niiyama, J. Ninkovic, N. K. Nisar,
 S. Nishida, K. Nishimura, M. H. A. Nouxman, B. Oberhof, K. Ogawa, S. Ogawa,
 S. L. Olsen, Y. Onishchuk, H. Ono, Y. Onuki, P. Oskin, F. Otani, E. R. Oxford, H. Ozaki,
 P. Pakhlov, G. Pakhlova, A. Paladino, T. Pang, A. Panta, E. Paoloni, S. Pardi,
 K. Parham, H. Park, S.-H. Park, B. Paschen, A. Passeri, A. Pathak, S. Patra, S. Paul,
 T. K. Pedlar, I. Peruzzi, R. Peschke, R. Pestotnik, F. Pham, M. Piccolo, L. E. Piilonen,
 G. Pinna Angioni, P. L. M. Podesta-Lerma, T. Podobnik, S. Pokharel, L. Polat, V. Popov,
 C. Praz, S. Prell, E. Prencipe, M. T. Prim, M. V. Purohit, H. Purwar, N. Rad,
 P. Rados, S. Raiz, A. Ramirez Morales, R. Rasheed, N. Rauls, M. Reif, S. Reiter,
 M. Remnev, I. Ripp-Baudot, M. Ritter, M. Ritzert, G. Rizzo, L. B. Rizzuto,
 S. H. Robertson, D. Rodríguez Pérez, J. M. Roney, C. Rosenfeld, A. Rostomyan,
 N. Rout, M. Rozanska, G. Russo, D. Sahoo, Y. Sakai, D. A. Sanders, S. Sandilya,
 A. Sangal, L. Santelj, P. Sartori, Y. Sato, V. Savinov, B. Scavino, C. Schmitt, M. Schnepf,
 M. Schram, H. Schreeck, J. Schueler, C. Schwanda, A. J. Schwartz, B. Schwenker,
 M. Schwickardi, Y. Seino, A. Selce, K. Senyo, I. S. Seong, J. Serrano, M. E. Sevier,
 C. Sfienti, V. Shebalin, C. P. Shen, H. Shibuya, T. Shillington, T. Shimasaki, J.-G. Shiu,
 B. Shwartz, A. Sibidanov, F. Simon, J. B. Singh, S. Skambraks, J. Skorupa, K. Smith,
 R. J. Sobie, A. Soffer, A. Sokolov, Y. Soloviev, E. Solovieva, S. Spataro, B. Spruck,
 M. Starič, S. Stefkova, Z. S. Stottler, R. Stroili, J. Strube, J. Stypula, R. Sugiura,
 M. Sumihama, K. Sumisawa, T. Sumiyoshi, D. J. Summers, W. Sutcliffe, S. Y. Suzuki,
 H. Svidras, M. Tabata, M. Takahashi, M. Takizawa, U. Tamponi, S. Tanaka, K. Tanida,
 H. Tanigawa, N. Taniguchi, Y. Tao, P. Taras, F. Tenchini, R. Tiwary, D. Tonelli,
 E. Torassa, N. Toutounji, K. Trabelsi, I. Tsaklidis, T. Tsuboyama, N. Tsuzuki, M. Uchida,
 I. Ueda, S. Uehara, Y. Uematsu, T. Ueno, T. Uglov, K. Unger, Y. Unno, K. Uno, S. Uno,
 P. Urquijo, Y. Ushiroda, Y. V. Usov, S. E. Vahsen, R. van Tonder, G. S. Varner,
 K. E. Varvell, A. Vinokurova, L. Vitale, V. Vobbiliseti, V. Vorobyev, A. Vossen, B. Wach,
 E. Waheed, H. M. Wakeling, K. Wan, W. Wan Abdullah, B. Wang, C. H. Wang,
 E. Wang, M.-Z. Wang, X. L. Wang, A. Warburton, M. Watanabe, S. Watanuki, J. Webb,
 S. Wehle, M. Welsch, C. Wessel, J. Wiechczynski, P. Wieduwilt, H. Windel, E. Won,

L. J. Wu, X. P. Xu, B. D. Yabsley, S. Yamada, W. Yan, S. B. Yang, H. Ye, J. Yelton, I. Yeo, J. H. Yin, M. Yonenaga, Y. M. Yook, K. Yoshihara, T. Yoshinobu, C. Z. Yuan, Y. Yusa, L. Zani, Y. Zhai, J. Z. Zhang, Y. Zhang, Y. Zhang, Z. Zhang, V. Zhilich, J. Zhou, Q. D. Zhou, X. Y. Zhou, V. I. Zhukova, V. Zhulanov, and R. Žlebčík

(Belle II Collaboration)

Abstract

We report measurements of the branching fraction (\mathcal{B}) and direct CP -violating asymmetry (\mathcal{A}_{CP}) of the charmless decay $B^0 \rightarrow K^0\pi^0$ at Belle II. A sample of e^+e^- collisions, corresponding to 189.8 fb^{-1} of integrated luminosity, recorded at the $\Upsilon(4S)$ resonance is used for the first decay-time-dependent analysis of these decays within the experiment. We reconstruct about 135 signal candidates, and measure $\mathcal{B}(B^0 \rightarrow K^0\pi^0) = [11.0 \pm 1.2(\text{stat}) \pm 1.0(\text{syst})] \times 10^{-6}$ and $\mathcal{A}_{CP}(B^0 \rightarrow K^0\pi^0) = -0.41_{-0.32}^{+0.30}(\text{stat}) \pm 0.09(\text{syst})$.

1. INTRODUCTION

The $B^0 \rightarrow K^0 \pi^0$ decay is mediated by flavor-changing neutral currents. In the standard model (SM), the dominant decay amplitude is given by the $b \rightarrow s \bar{d} \bar{d}$ loop, which is dominated by the top quark contribution and carries a weak phase $\arg(V_{tb} V_{ts}^*)$. Here, V_{ij} denote the CKM matrix elements. Such processes are suppressed in the SM and provide an indirect route to search for beyond-the-SM particles that might be exchanged in the loop. In the $B^0 \rightarrow K^0 \pi^0$ decay, CP violation can occur either directly in the decay amplitude (\mathcal{A}_{CP}) or via the interference between decays with and without B^0 - \bar{B}^0 mixing (\mathcal{S}_{CP}). Neglecting subleading contributions to the amplitude, \mathcal{S}_{CP} is expected to be equal to $\sin 2\phi_1$ and $\mathcal{A}_{CP} \approx 0$, where $\phi_1 \equiv \arg(-V_{cd} V_{cb}^*/V_{td} V_{tb}^*)$. Deviations from these expectations could be due to larger-than-expected subleading SM contributions or from non-SM physics.

Combining B -meson lifetimes (τ) with branching fractions (\mathcal{B}) and direct CP asymmetries of four $B \rightarrow K\pi$ decays related by isospin symmetry, the sum rule proposed in Ref. [1],

$$\begin{aligned} & \mathcal{A}_{CP}(K^+ \pi^-) + \mathcal{A}_{CP}(K^0 \pi^+) \frac{\mathcal{B}(K^0 \pi^+) \tau_{B^0}}{\mathcal{B}(K^+ \pi^-) \tau_{B^+}} \\ & - 2\mathcal{A}_{CP}(K^+ \pi^0) \frac{\mathcal{B}(K^+ \pi^0) \tau_{B^0}}{\mathcal{B}(K^+ \pi^-) \tau_{B^+}} - 2\mathcal{A}_{CP}(K^0 \pi^0) \frac{\mathcal{B}(K^0 \pi^0)}{\mathcal{B}(K^+ \pi^-)} = 0, \end{aligned} \quad (1)$$

is expected to hold with an uncertainty below 1% and provides an important consistency test of the SM. Deviations from this isospin sum rule can be caused by an enhancement of color-suppressed tree amplitudes, or by contributions from non-SM physics. The prediction of the CP asymmetry $\mathcal{A}_{CP}(K^0 \pi^0)$ from this sum-rule is -0.138 ± 0.025 [2], using up-to-date known values of other quantities [3]. Combining measurements from Belle and BaBar [4, 5], the Heavy Flavor Averaging Group finds $\mathcal{A}_{CP} = 0.01 \pm 0.10$ [3]. The dominant contribution to the uncertainty in this sum-rule comes from the uncertainty in $\mathcal{A}_{CP}(K^0 \pi^0)$. Therefore, a precise measurement of $\mathcal{A}_{CP}(K^0 \pi^0)$ is crucial for this consistency test of the SM.

Preliminary results on \mathcal{B} and \mathcal{A}_{CP} of $B^0 \rightarrow K^0 \pi^0$ decays have been reported by Belle II using a data sample corresponding to 62.8 fb^{-1} . In this analysis, we utilize a larger data set (189.8 fb^{-1}) and further enhance our sensitivity to \mathcal{A}_{CP} by using B decay-time information.

At Belle II, pairs of neutral B mesons are coherently produced in the process $e^+ e^- \rightarrow \Upsilon(4S) \rightarrow B^0 \bar{B}^0$. When one of the B mesons decays to a CP eigenstate f_{CP} , such as $K_s^0 \pi^0$, and the other to a flavor-specific final state f_{tag} , the time-dependent decay rate is given by

$$\mathcal{P}(\Delta t) = \frac{e^{-|\Delta t|/\tau_{B^0}}}{4\tau_{B^0}} [1 + q\{\mathcal{A}_{CP} \cos(\Delta m_d \Delta t) + \mathcal{S}_{CP} \sin(\Delta m_d \Delta t)\}], \quad (2)$$

where $\Delta t = t_{CP} - t_{\text{tag}}$ is the proper-time difference between the decays into f_{CP} and f_{tag} , q equals +1 (-1) for the B^0 (\bar{B}^0) decay to f_{tag} , and Δm_d is the B^0 - \bar{B}^0 mixing frequency. This analysis employs a decay-time-dependent CP asymmetry fit similar to the previous measurement of $\sin 2\phi_1$ [6]. The key challenge here lies in the determination of the position of the $B^0 \rightarrow K^0 \pi^0$ decay vertex. For that, the K_s^0 flight direction is projected back to the interaction region and the K_s^0 is required to decay inside the vertex detector (VXD). The full analysis was developed and tested with simulated data, and validated with data control samples before selecting and inspecting the $B^0 \rightarrow K^0 \pi^0$ candidates. Due to the limited sensitivity provided by the available data sample, we measure \mathcal{A}_{CP} by fixing \mathcal{S}_{CP} , Δm_d , and τ_{B^0} to their known values [3].

2. THE BELLE II DETECTOR AND DATA SAMPLE

Belle II [7] is a particle spectrometer having almost 4π solid-angle coverage, designed to reconstruct final-state particles of e^+e^- collisions delivered by the SuperKEKB asymmetric-energy collider [8]. It is located at the KEK laboratory in Tsukuba, Japan. The energies of the positron and electron beams are 4 and 7 GeV, respectively. Belle II consists of a number of subdetectors surrounding the interaction region in a cylindrical geometry. The innermost one is the VXD, comprised of several position-sensitive silicon sensors. It samples the trajectories of charged particles (‘tracks’) in the vicinity of the interaction region to determine the decay positions of their parent particles. The VXD includes two inner layers of pixel sensors and four outer layers of double-sided microstrip sensors. The second pixel layer is currently incomplete covering one sixth of the azimuthal angle. Charged-particle momenta and charges are measured by a large-radius, small-cell, central drift chamber (CDC), which also offers particle-identification information via a measurement of specific ionization. A Cherenkov-light angle and time-of-propagation detector surrounding the CDC provides charged-particle identification in the central detector volume, supplemented by proximity-focusing, aerogel, ring-imaging Cherenkov detectors in the forward region with respect to the electron beam. A CsI(Tl)-crystal electromagnetic calorimeter (ECL) provides energy measurements of electrons and photons. A solenoid surrounding the ECL generates a uniform axial 1.5 T magnetic field. Layers of plastic scintillators and resistive-plate chambers, interspersed between the magnetic flux-return iron plates, allow for the identification of K_L^0 mesons and muons. The subdetectors most relevant for our study are the VXD, CDC, and ECL.

We analyse collision data collected at a center-of-mass (CM) energy near the $\Upsilon(4S)$ resonance, corresponding to an integrated luminosity of 189.8 fb^{-1} . We use large samples of simulated $e^+e^- \rightarrow q\bar{q}$ ($q = u, d, s, c$), $\Upsilon(4S) \rightarrow B^0\bar{B}^0$ and B^+B^- events to optimize the event selection and study possible background contributions. Simulated $B^0 \rightarrow K_s^0\pi^0$ signal events are used to determine signal models and estimate the selection efficiency. We use the EVTGEN package [9] to generate B -mesons decays and the PHOTOS package [10] to calculate final-state radiation from all charged particles. The simulation of $e^+e^- \rightarrow q\bar{q}$ continuum background relies on the KKMC generator [11] interfaced to PYTHIA [12]. The interactions of final-state particles with the detector are simulated using GEANT4 [13].

3. RECONSTRUCTION AND SELECTION

Tracks are reconstructed with the VXD and CDC. Photons are identified as isolated energy clusters in the ECL that are not matched to any track. Candidate K_s^0 mesons are reconstructed from pairs of oppositely-charged particles with the dipion mass between 482 and $513 \text{ MeV}/c^2$. We reconstruct π^0 candidates from pairs of photons that have energies greater than 80 (223) MeV if detected in the barrel (endcap) ECL. We apply the different energy thresholds to suppress beam background, which is higher in the endcap compared to the barrel region. The selection also requires the diphoton mass to lie between 119 and $150 \text{ MeV}/c^2$ and the absolute value of the cosine of the angle between each photon and the B meson in the π^0 rest frame to be less than 0.953. These criteria suppress contributions from misreconstructed π^0 candidates.

A B -meson candidate is reconstructed by combining a K_s^0 with a π^0 candidate. For this purpose, we use two kinematic variables, the beam-energy-constrained mass (M_{bc}) and the

energy difference (ΔE),

$$\begin{aligned} M_{\text{bc}} &= \sqrt{E_{\text{beam}}^2 - \vec{p}_B^2}, \\ \Delta E &= E_B - E_{\text{beam}}, \end{aligned} \quad (3)$$

where E_{beam} is the beam energy, and E_B and \vec{p}_B are respectively the reconstructed energy and momentum of the B meson; all calculated in the CM frame.

The presence of a high momentum π^0 causes a significant correlation between M_{bc} and ΔE due to the shower leakage of final-state photons. To reduce this correlation, we use a modified version of M_{bc} that is defined in terms of the beam energy and momenta of final-state particles as

$$M'_{\text{bc}} = \sqrt{E_{\text{beam}}^2 - \left(\vec{p}_{K_S^0} + \frac{\vec{p}_{\pi^0}}{|\vec{p}_{\pi^0}|} \sqrt{(E_{\text{beam}} - E_{K_S^0})^2 - m_{\pi^0}^2} \right)^2}, \quad (4)$$

where all kinematic quantities are again calculated in the CM frame. We retain candidate events satisfying $5.24 < M'_{\text{bc}} < 5.29$ GeV/ c^2 and $|\Delta E| < 0.30$ GeV.

To measure the proper-time difference Δt , we need to determine the signal and tag-side B decay vertices. The signal B vertex is obtained by projecting the flight direction of the K_S^0 candidate back to the interaction region. The K_S^0 flight direction is determined from its decay vertex and momentum. The intersection of the K_S^0 -flight projection with the interaction region provides a good approximation of the signal B decay vertex, since both the transverse flight length of the B^0 meson and the transverse size of the interaction region are small compared to the B^0 flight length along the boost direction. The tag-side vertex is obtained with tracks that are not associated to the $B^0 \rightarrow K_S^0 \pi^0$ decay. We obtain Δt by dividing the longitudinal distance between the signal and tag vertices by the speed of light and the Lorentz boost of the $\Upsilon(4S)$ system in the lab frame. Signal candidates with poorly measured Δt , mainly due to K_S^0 mesons decaying outside of the VXD acceptance, are suppressed by requiring the estimated uncertainty on Δt to be less than 2.5 ps.

Events from continuum $e^+e^- \rightarrow q\bar{q}$ production are suppressed using a boosted-decision-tree (BDT) classifier [14] that exploits several event-topology variables known to provide discrimination between B -meson signal and continuum background. The following variables are those offering most of the discrimination: modified Fox–Wolfram moments [15], CLEO cones [16], the magnitude of the thrust axis for the reconstructed B candidate, and the cosine of the angle between the thrust axis of the signal B and that of rest of event. The BDT is trained on samples of simulated $e^+e^- \rightarrow q\bar{q}$, $B^0\bar{B}^0$ and B^+B^- events, each equivalent to an integrated luminosity of 1 ab^{-1} . The BDT output distribution (C_{out}) is shown in Fig. 1. We apply a criterion $C_{\text{out}} > 0.60$, which rejects about 89% of the continuum background with a 18% relative loss in signal efficiency. We then translate C_{out} into a new variable,

$$C'_{\text{out}} = \ln \left(\frac{C_{\text{out}} - C_{\text{out,min}}}{C_{\text{out,max}} - C_{\text{out}}} \right), \quad (5)$$

where $C_{\text{out,min}} = 0.60$ and $C_{\text{out,max}} = 0.99$. The distributions of C'_{out} can be parametrized with Gaussian functions.

After applying all selection criteria, the average number of B candidates per event is 1.009. Multiple candidates arise due to random combinations of final-state particles. To select the best combination in an event with multiple candidates, we first compare the

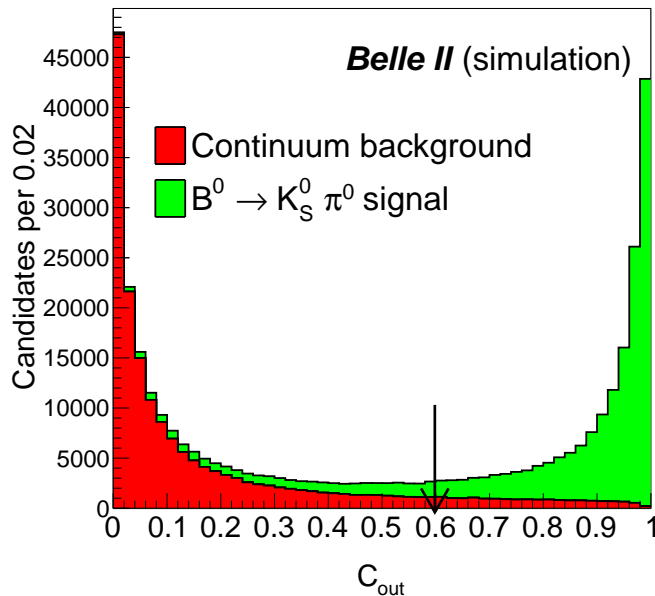


FIG. 1. Distributions of the BDT output C_{out} for simulated signal and $e^+e^- \rightarrow q\bar{q}$ events. The downward arrow indicates the position of the applied C_{out} selection.

π^0 mass-constrained fit χ^2 probability (‘p-value’). If there are two or more B candidates sharing the same π^0 , we choose the one with the best p-value of the fit of the K_S^0 vertex. This selection retains the correct B candidate in 74% of simulated signal events.

The signal efficiency (ϵ) of correctly reconstructed events after all selection criteria have been applied is 12.3%. From simulation we find that signal candidates can be incorrectly reconstructed in 1.5% of the times by accidentally picking up a particle from the other B meson decay.

We determine the flavor of the tag-side B meson (q) from the properties of the final-state particles that are not associated with the reconstructed $B^0 \rightarrow K_S^0 \pi^0$ decay. The Belle II multivariate flavor-tagger algorithm [17] uses the information of B -decay products to determine the quark-flavor of B mesons. It gives two parameters, the b -flavor charge, q and its quality factor r . The parameter r is an event-by-event, MC determined flavour-tagging dilution factor that ranges from 0 (no flavor discrimination) to 1 (unambiguous flavor assignment).

4. DETERMINATION OF BRANCHING FRACTION AND CP ASYMMETRY

We obtain the signal yield and direct CP asymmetry from an extended maximum-likelihood fit to the unbinned distributions of M'_{bc} , ΔE , C'_{out} , and Δt . For the signal component, M'_{bc} is modeled with the sum of a Crystal Ball [18] and a Gaussian function with a common mean; ΔE with the sum of a Crystal Ball and two Gaussian functions, all three with a common mean; and C'_{out} with the sum of an asymmetric and a regular Gaussian

function. The signal Δt probability density function (PDF) is given by

$$\mathcal{P}_{\text{sig}}(\Delta t, q) = \frac{e^{-|\Delta t|/\tau_{B^0}}}{4\tau_{B^0}} [\{1 - q\Delta w_r + q\mu_r(1 - 2w_r)\} + \{q(1 - 2w_r) + \mu_r(1 - q\Delta w_r)\}] \quad (6)$$

$$\{\mathcal{A}_{CP} \cos(\Delta m_d \Delta t) + \mathcal{S}_{CP} \sin(\Delta m_d \Delta t)\} \otimes \mathcal{R}_{\text{sig}},$$

where w_r is the fraction of incorrectly tagged events, Δw_r is the difference in w_r between B^0 and \bar{B}^0 , μ_r is the difference in their tagging efficiency (that is the fraction of signal B^0 or \bar{B}^0 candidates to which a flavor tag can be assigned), and \mathcal{R}_{sig} is the Δt resolution function. The function \mathcal{R}_{sig} is composed of a sum of two Gaussians with a combined width of ≈ 0.9 ps, and its parameters are determined with simulated events. We set τ_{B^0} to 1.520 ps, Δm_d to 0.507 ps^{-1} , and \mathcal{S}_{CP} to 0.57 [3]. The data are divided into seven $q \times r$ bins with the tagging parameters for each bin (w_r , Δw_r , and μ_r) fixed to the corresponding values [17]. The effective tagging efficiency ϵ_{eff} ($= \sum_r \epsilon_r \times (1 - 2w_r)^2$, where ϵ_r is the partial effective efficiency in the r -th bin), w_r , and μ_r are $(30.0 \pm 1.2)\%$, $(2-47)\%$, and $(0.5-11)\%$, respectively. All signal PDF shapes are fixed to the values determined from a $q \times r$ binned fit to simulated events.

For the continuum background component, an ARGUS function [19] is used for M'_{bc} , a linear function for ΔE , and the sum of an asymmetric and a regular Gaussian function for C'_{out} . Its Δt distribution is modeled with an exponential function convolved with a Gaussian for the tail; we use a double Gaussian for its resolution function ($\mathcal{R}_{q\bar{q}}$). For the continuum background component, we float the PDF shape parameters, which are found to be common for all $q \times r$ bins. For the $B\bar{B}$ background component, a two-dimensional Kernel estimation PDF [20] is used to model the ΔE vs. M'_{bc} distribution, and the sum of an asymmetric and a regular Gaussian function is used for C'_{out} . Its Δt distribution is modeled with an exponential function convolved with a Gaussian for the tail; we again use a double Gaussian for its resolution function ($\mathcal{R}_{B\bar{B}}$). The $B\bar{B}$ background shape parameters are fixed from a fit to the corresponding simulated sample.

The fit parameters are the signal yield N_{sig} ; \mathcal{A}_{CP} ; $B\bar{B}$ background yield, which is Gaussian constrained to the result of a fit to the ΔE sideband in data; continuum background yield; M'_{bc} ARGUS parameter; ΔE slope; and effective width of C'_{out} for the $q\bar{q}$ component. We correct the signal M'_{bc} , ΔE , and C'_{out} PDF shapes for possible data–simulation differences, according to the values obtained with a control sample of $B^+ \rightarrow \bar{D}^0 (\rightarrow K^+ \pi^- \pi^0) \pi^+$ (charge conjugated modes are implicitly included hereafter). In order to mimic the signal decay, we apply a similar π^0 selection. We use a maximum-likelihood fit to the unbinned distributions of M'_{bc} , ΔE , and C'_{out} , using PDF shapes similar to those employed to describe the signal in data. We use a control sample of $B^0 \rightarrow J/\psi (\rightarrow \mu^+ \mu^-) K_S^0$ decays to validate the time-dependent analysis. To mimic the signal decay, we do not use the two muons coming from the J/ψ to reconstruct the signal B decay vertex. We use a maximum-likelihood fit to the unbinned distributions of M_{bc} and Δt , using PDF shapes and resolution functions similar to those employed in the fit to the signal in data. The B^0 lifetime and \mathcal{A}_{CP} are measured to be $1.59_{-0.08}^{+0.09}$ ps and -0.03 ± 0.10 , respectively, which are consistent with their known values [3]. The uncertainties quoted here are statistical only. This provides convincing data-driven support for the time-dependent part of the analysis. The same sample is also used to correct the Δt PDF shape parameters for possible data–simulation differences. The estimator properties (mean and uncertainty) have been studied in both simplified and realistic simulated experiments and found to be as expected.

Figure 2 shows the four projections of the fit to the seven $q \times r$ -integrated data samples which include both B^0 and \bar{B}^0 candidates. For each projection the signal enhancing criteria, $5.27 < M'_{bc} < 5.29 \text{ GeV}/c^2$, $-0.15 < \Delta E < 0.10 \text{ GeV}$, $|\Delta t| < 10.0 \text{ ps}$, and $C'_{\text{out}} > 0.0$, are applied on all except for the variable displayed. The obtained signal yield is 135_{-15}^{+16} , where the quoted uncertainty is statistical only. We also find 2214_{-48}^{+49} continuum and 44 ± 5 $B\bar{B}$ background events. We determine the branching fraction using the following formula:

$$\mathcal{B}(B^0 \rightarrow K^0 \pi^0) = \frac{N_{\text{sig}}}{2 \times N_{B\bar{B}} \times f^{00} \times \epsilon \times \mathcal{B}_s}, \quad (7)$$

where $N_{B\bar{B}} = (197.2 \pm 5.70) \times 10^6$, $f^{00} = 0.487 \pm 0.010$ [21], and $\mathcal{B}_s = 0.5$ are the number of $B\bar{B}$ pairs, $\mathcal{Y}(4S) \rightarrow B^0 \bar{B}^0$ branching fraction, and $K^0 \rightarrow K_s^0$ branching fraction, respectively. The $B^0 \rightarrow K^0 \pi^0$ branching fraction and direct CP asymmetry (\mathcal{A}_{CP}) are measured to be $(11.0 \pm 1.2 \pm 1.0) \times 10^{-6}$ and $-0.41_{-0.32}^{+0.30} \pm 0.09$, respectively. The first uncertainties are statistical and the second is systematic (described in Section 5). This extends the previous measurement [22] of \mathcal{B} and \mathcal{A}_{CP} in $B^0 \rightarrow K^0 \pi^0$ decays, where no information on the proper-time difference was used.

5. SYSTEMATIC UNCERTAINTIES

The various systematic uncertainties contributing to \mathcal{B} and \mathcal{A}_{CP} are listed in Table I. Assuming these sources to be independent, we add their contributions in quadrature to obtain the total systematic uncertainty. The systematic uncertainty due to possible differences between data and simulation in the reconstruction of charged particles is 0.3% per track [23]. We linearly add this uncertainty in \mathcal{B} for each of the two pion tracks coming from the decay of the K_s^0 in the signal B . From a comparison of the K_s^0 yield in data and simulation, we find that the ratio of the K_s^0 reconstruction efficiency changes approximately as a linear function of its flight length [23]. We apply an uncertainty of 0.4% for each centimeter of the average flight length of the K_s^0 candidates resulting in a 4.2% total systematic uncertainty in \mathcal{B} . We estimate the systematic uncertainty due to possible differences between data and simulation in the π^0 reconstruction and selection by comparing the inclusive decay sample of $D^0 \rightarrow K^- \pi^+ \pi^0$ with $D^0 \rightarrow K^- \pi^+$ [24]. The data-simulation efficiency ratio is found to be close to unity with an uncertainty of 7.5%, which we assign as a systematic uncertainty in \mathcal{B} . We evaluate possible data-simulation differences in the continuum-suppression efficiency using the control sample of $B^+ \rightarrow \bar{D}^0 (\rightarrow K^+ \pi^- \pi^0) \pi^+$. As the ratio of efficiencies obtained in data and simulation is close to unity, the statistical uncertainty in the ratio (1.6%) is assigned as a systematic uncertainty to \mathcal{B} . We estimate the systematic uncertainty in \mathcal{A}_{CP} due to the uncertainty in the wrong-tag fraction by varying the parameter individually for each $q \times r$ region by its uncertainty. The systematic uncertainty due to the Δt resolution function is estimated in a similar fashion. As external inputs τ_{B^0} , Δm_d , and \mathcal{S}_{CP} are fixed to their known values in the fit, the associated systematic uncertainties are estimated by varying the values by their uncertainties. In the nominal fit, we assume the $B\bar{B}$ -background decays to be CP symmetric. To account for a potential CP asymmetry in the $B\bar{B}$ background, we use an alternative Δt PDF given by

$$\mathcal{P}_{B\bar{B}}(\Delta t, q) = \frac{e^{-|\Delta t|/\tau_{B^0}}}{4\tau_{B^0}} [1 + q\{\mathcal{A}'_{CP} \cos(\Delta m_d \Delta t) + \mathcal{S}'_{CP} \sin(\Delta m_d \Delta t)\}] \otimes R_{B\bar{B}}. \quad (8)$$

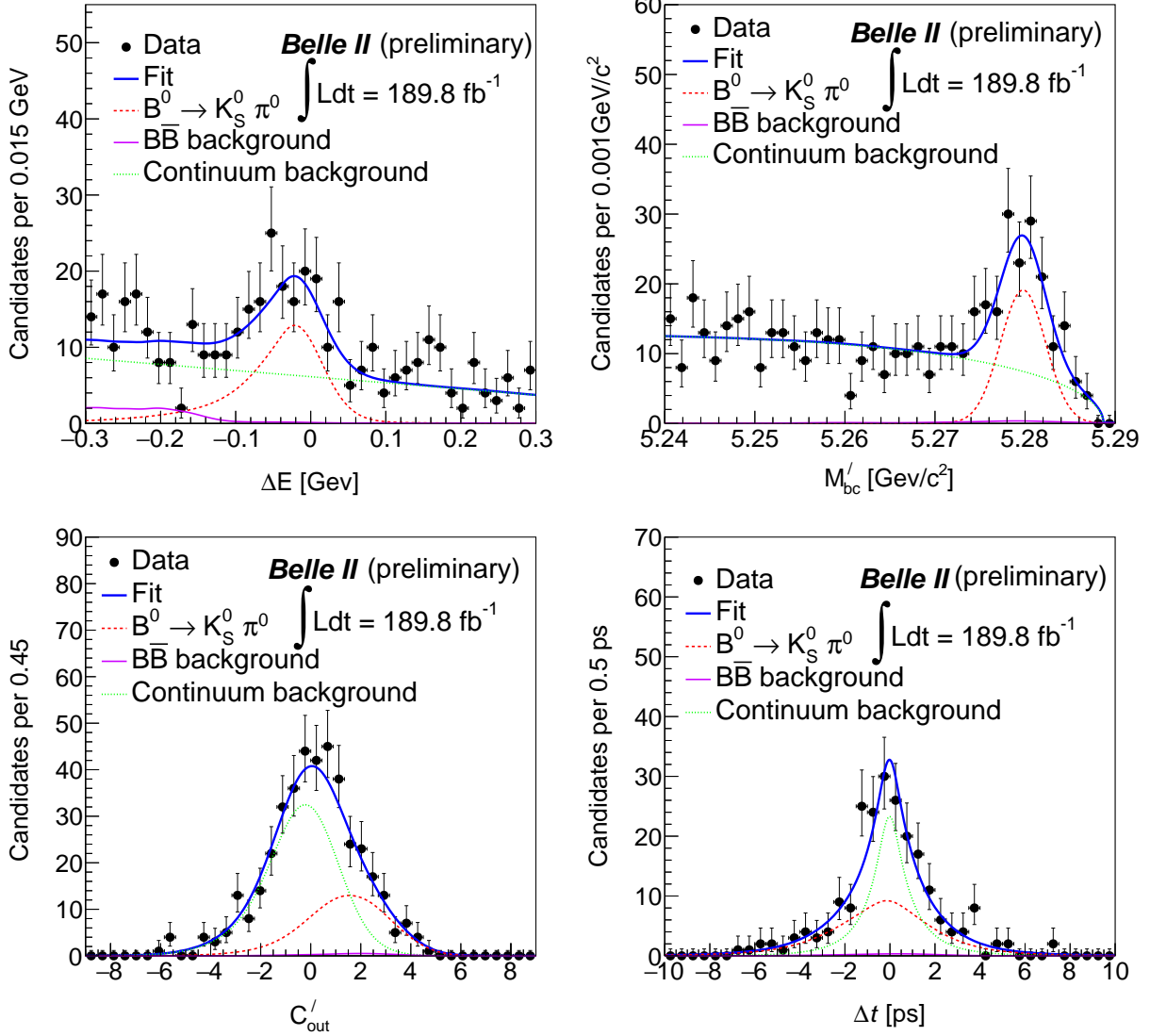


FIG. 2. Signal enhanced fit projections of ΔE (upper-left), M'_{bc} (upper-right), C'_{out} (lower-left), and Δt (lower-right) shown for the data sample integrated in the seven $q \times r$ bins.

We perform fits to simplified simulated experiments by varying \mathcal{S}'_{CP} and \mathcal{A}'_{CP} from +1 to -1. We then calculate the deviations in signal \mathcal{A}_{CP} from its nominal value. These deviations are assigned as a systematic uncertainty to \mathcal{A}_{CP} due to the asymmetry of the $B\bar{B}$ background. An overall uncertainty of 3.2% in \mathcal{B} is taken as a systematic uncertainty due to the number of $B\bar{B}$ pairs used, which also includes the uncertainty in f^{00} . The uncertainties due to the signal PDF shape parameters are estimated by varying their uncertainties. Similarly, the uncertainties due to the background PDF shape are calculated by varying all fixed parameters by their uncertainties, determined from the fit to simulated samples. We fix the M'_{bc} ARGUS endpoint to the value obtained from a fit to the ΔE sideband data. Subsequently we vary it by $\pm 1\sigma$ to assign a systematic uncertainty, where σ is the uncertainty from the fit. A potential fit bias is checked by performing an ensemble test comprising 1000 simplified simulated experiments in which signal events are drawn from the corresponding simulation

sample and background events are generated according to their PDF shapes. We calculate the mean shift of the signal yield from the input value and assign it as a systematic uncertainty. Tag-side interference can arise due to the presence of both CKM-favored and -suppressed tree amplitudes. The systematic uncertainty in \mathcal{A}_{CP} assigned to this interference is taken from Ref. [6]. A possible systematic uncertainty related to VXD misalignment is neglected in this study.

TABLE I. List of systematic uncertainties contributing to the branching fraction and direct CP asymmetry.

Source	$\delta\mathcal{B}$ (%)	$\delta\mathcal{A}_{CP}$
Tracking efficiency	0.6	–
K_s^0 reconstruction efficiency	4.2	–
π^0 reconstruction efficiency	7.5	–
Continuum suppression efficiency	1.6	–
Number of $B\bar{B}$ pairs	3.2	–
Flavor tagging	–	0.040
Resolution function	–	0.050
External inputs	0.4	0.021
$B\bar{B}$ background asymmetry	–	0.002
Signal modelling	1.0	0.015
Background modelling	0.9	0.004
Possible fit bias	2.0	0.010
Tag-side interference	–	0.038
Total	9.6	0.086

6. SUMMARY

We report measurements of the branching fraction and direct CP asymmetry in $B^0 \rightarrow K^0\pi^0$ decays using a data sample, corresponding to 189.8fb^{-1} of integrated luminosity, recorded by Belle II at the $\Upsilon(4S)$ resonance. The observed signal yield is 135_{-15}^{+16} . We measure $\mathcal{B}(B^0 \rightarrow K^0\pi^0) = [11.0 \pm 1.2(\text{stat}) \pm 1.0(\text{syst})] \times 10^{-6}$ and $\mathcal{A}_{CP} = -0.41_{-0.32}^{+0.30}(\text{stat}) \pm 0.09(\text{syst})$. This is the first measurement of \mathcal{A}_{CP} in $B^0 \rightarrow K^0\pi^0$ performed at Belle II using a decay-time-dependent analysis. The results agree with previous determinations [3, 22].

7. ACKNOWLEDGEMENT

We thank the SuperKEKB group for the excellent operation of the accelerator; the KEK cryogenics group for the efficient operation of the solenoid; and the KEK computer group for on-site computing support.

-
- [1] M. Gronau, *Phys. Lett. B* **627**, 82 (2005).
 - [2] R. Aaij et al. (LHCb Collaboration), *Phys. Rev. Lett.* **126**, 091802 (2021).
 - [3] Y. Amhis et al. (Heavy Flavor Averaging Group), *Eur. Phys. J. C* **81**, 226 (2021), arXiv:1909.12524.
 - [4] M. Fujikawa et al. (Belle Collaboration), *Phys. Rev. D* **81**, 011101 (2010).
 - [5] B. Aubert et al. (BaBar Collaboration), *Phys. Rev. D* **79**, 052003 (2009).
 - [6] I. Adachi et al. (Belle Collaboration), *Phys. Rev. Lett.* **108**, 171802 (2012).
 - [7] T. Abe et al. (Belle II Collaboration), KEK Report 2010-1, arXiv:1011.0352.
 - [8] K. Akai, K. Furukawa, and H. Koiso (SuperKEKB Group), *Nucl. Instrum. Meth. A* **907**, 188 (2018).
 - [9] D. Lange, *Nucl. Instrum. Meth. A* **462**, 152 (2001).
 - [10] E. Barberio, B. van Eijk, and Z. Was, *Comp. Phys. Comm.* **66**, 115 (1991).
 - [11] B. Ward, S. Jadach, and Z. Was, *Nucl. Phys. B Proc. Suppl.* **116**, 73 (2003)
 - [12] T. Sjöstrand, S. Mrenna, and P. Skands, *Comp. Phys. Comm.* **178**, 852 (2008).
 - [13] S. Agostinelli et al. (GEANT4 Collaboration), *Nucl. Instrum. Meth. A* **506**, 250 (2003).
 - [14] T. Keck, arXiv:1609.06119.
 - [15] G. C. Fox and S. Wolfram, *Phys. Rev. Lett.* **41**, 1581 (1978).
 - [16] D. M. Asner et al. (CLEO Collaboration), *Phys. Rev. D* **53**, 1039 (1996).
 - [17] F. Abudinén et al. (Belle II Collaboration), *Eur. Phys. J. C* **82**, 283 (2022).
 - [18] T. Skwarnicki, PhD thesis, INP Krakow, DESY-F31-86-02 (1986).
 - [19] H. Albrecht et al. (ARGUS Collaboration), *Phys. Lett. B* **241**, 278 (1990).
 - [20] K. S. Cranmer, *Comp. Phys. Comm.* **136**, 198 (2001).
 - [21] B. Aubert et al. (BaBar Collaboration), *Phys. Rev. Lett.* **95**, 042001 (2005).
 - [22] F. Abudinén et al. (Belle II Collaboration), BELLE2-CONF-PH-2021-001, arXiv:2104.14871.
 - [23] V. Bertacchi et al. (Belle II Tracking Group), *Comp. Phys. Comm.* **259**, 107610 (2021).
 - [24] G. Bonvicini et al. (CLEO Collaboration), *Phys. Rev. D* **89**, 072002 (2014).
 - [25] L. Šantelj et al. (Belle Collaboration), *JHEP* **10**, 165 (2014).